



Original contribution

# Magnetic resonance imaging in the presence of projectiles and projectile fragments: Artefacts, image quality, rotation and movement

Hackenbroch C.<sup>a,\*</sup>, Wafa M.<sup>a</sup>, Klinger S.<sup>b</sup>, Mauer U.M.<sup>b</sup><sup>a</sup> Department of Radiology, German Armed Forces Hospital of Ulm, Germany<sup>b</sup> Department of Neurosurgery, German Armed Forces Hospital of Ulm, Germany

## ARTICLE INFO

## Keywords:

MRI  
Safety  
Projectiles  
Artefacts  
Gunshot injuries

## ABSTRACT

**Background and purpose:** Gunshot injuries have been considered a contraindication for MRI because of the risk of secondary dislodgement of retained metallic foreign bodies.

The objective of our study was to provide a systematic overview of the behaviour of projectiles and fragments in order to aid decision-making regarding the use of MRI in clinical practice.

**Materials and methods:** Ferromagnetic (n = 2) and non-ferromagnetic (n = 5) projectiles and fragments that were lodged in soft tissue (porcine masseter muscles) were examined using standard protocols at 1, 1.5 and 3 T, to simulate clinical situations as realistically as possible. CT was performed before and after every MRI to assess rotation and movement. Artefacts and image quality were analysed using Likert-type scales.

**Results:** Ferromagnetic projectiles were of poorer quality and showed larger artefacts and did not provide benefit for clinical practice compared to images of non-ferromagnetic material. Image quality of non-ferromagnetic projectiles varied widely (from very good to moderate) depending on the composition of the projectiles.

Field strength (1 T to 3 T) had no relevant influence on image quality.

**Conclusions:** Non-ferromagnetic projectiles are not a contraindication for MR imaging since there is no potential risk of secondary dislodgement. Image quality and the extent of artefacts, however, strongly depend on the type of ammunition used. The presence of ferromagnetic projectiles in or near vital anatomic structures is a contraindication for MRI because these objects may exhibit movement in response to magnetic fields. Knowledge of the type of projectile used appears to be important in order to guide patient management before an examination is performed. So, the production and use of projectiles suitable for MRI should be favored in the future, knowing that this will be hard to fulfil.

## 1. Introduction

Gunshot injuries associated with projectiles or projectile fragments that remain embedded in the body occur not only during military operations but also in law enforcement, hunting, sports and criminal settings. [1,10]

The Federal Statistical Office of Germany reported that an average of approximately 70 people die in Germany every year as a result of attacks and accidents involving the use of guns. [9]

Emergency medical services in Germany have continuously improved in recent years. Shorter patient transportation times, the continuous further development of medical equipment and the availability of well-trained personnel have led to lower mortality rates and better clinical outcomes for patients. [13] As a result, secondary procedures for the diagnosis and management of sequelae and residual lesions play

an increasingly important role.

Whereas computed tomography, radiography and ultrasound are used in the acute management of patients, MRI is the imaging modality of choice for the secondary evaluation of soft-tissue injuries.

MRI is limited by ferromagnetic attraction, which can result not only in artefacts of varying severity but may also cause the displacement of magnetic projectiles and fragments. This leads to the risk of iatrogenic damage to surrounding tissues.

Available studies investigated the rotation of projectiles in gel and gelatin blocks and included only a few MRI sequences. These demonstrated considerable rotation and dislodgement of projectiles.

## 2. Methods

Projectiles and projectile fragments were placed in masseter muscles

\* Corresponding author at: Department of Radiology, German Armed Forces Hospital of Ulm, Oberer Eselsberg 40, 89081 Ulm, Germany.

E-mail address: [carstenhackenbroch@bundeswehr.org](mailto:carstenhackenbroch@bundeswehr.org) (C. Hackenbroch).

**Table 1**  
Overview of the projectiles used.

| Projectile                   | Manufacturer     | Calibre in mm | Composition                           | Weight of projectile in g | Weight of fragments in g | Type of gun            | Type of projectile | Use  | Magnetism (in degrees; measured during the tests with a protractor) |
|------------------------------|------------------|---------------|---------------------------------------|---------------------------|--------------------------|------------------------|--------------------|--|---|
| Sintox Action 4              | RUAG             | 9 × 19        | Copper alloy, solid                   | 6.184                     | 2.273                    | Pistol, submachine gun | Semi-jacketed      | Police, special weapons and tactics (SWAT) teams | Low level (5°)  |
| Speer Gold Dot               | Speer            | 9 × 19        | Copper, solid                         | 8.039                     | 2.861                    | Pistol                 | Hollow point       | Hunters, police                                  | No (0°)   |
| Zombie Max                   | Hornady          | 9 × 19        | Copper jacket, lead core              | 7.442                     | 1.686                    | Revolver               | Hollow point       | Hunters  | No (0°)   |
| Magtech, 9 mm Luger          | Magtech          | 9 × 19        | Copper jacket, lead core              | 8.002                     | 1.817                    | Pistol                 | Fully jacketed     | Hunters  | No (0°)   |
| MEN PEP 2.0                  | MEN              | 9 × 19        | Copper, solid                         | 5.923                     | 5.814                    | Pistol                 | Semi-jacketed      | Police   | No (0°)   |
| Sellier & Bellot, 9 mm Luger | Sellier & Bellot | 9 × 19        | Lead, solid                           | 7.945                     | –                        | Pistol                 | Lead, round-nosed  | Hunters  | No (0°)   |
| Sintox Standard              | RUAG             | 9 × 19        | Nickel-plated steel jacket, lead core | 7.955                     | 5.839                    | Pistol, submachine gun | Fully jacketed     | Police, SWAT teams, German armed forces          | High level (90°)  |

of domestic pigs in order to simulate their presence in human tissue. These projectiles and fragments were then evaluated on different MRI sequences at field strengths of 1 Tesla (T), 1.5 T and 3 T. Computed tomography (CT) scans were obtained before and after MRI examinations in order to assess and compare the locations of projectiles and fragments.

We studied seven different projectiles (9 × 19 mm calibre) and fragments of these projectiles, which are commonly used in military, law enforcement, sports and hunting settings. Prior to the first examination, the ferromagnetic properties of every projectile were assessed as described by Hess and Harms [6].

The types of projectiles are given in Table 1 and Fig. 1.

We fired projectiles in a standardised fashion at a steel plate from a distance of 25 m in order to obtain projectile fragments. The only exception was a lead round-nosed 9 mm Luger manufactured by Sellier & Bellot. When fired, this projectile did not fragment but remained intact.

A standardised protocol, which consisted of twelve tests, was established for preparing and examining the porcine heads. Movement of the projectiles and their fragments was defined as any misalignment compared to the initial CT-scan, regardless distance of displacement or degree of rotation. The order of tests and the used projectiles are given in Table 2.

Table 3 provides an overview of the exact sequence parameters of the 1-T, 1.5-T and 3-T scanners. Standard protocols for MRI of the skull after traumatic brain injuries were used.

Based on the analysis by Hess et al. [6], we established a rating scale for assessing artefacts and used it to evaluate artefacts on the various sequences.

> Classification of artefacts depending on size

- 1 = less than 1 cm
- 2 = 1 to 3 cm
- 3 = 3 to 5 cm
- 4 = more than 5 cm

> Assessment of image quality

- A = good
- B = moderate (of limited use)
- C = poor (of no use)

### 3. Results

#### 3.1. Movement

Post-MRI CT examinations showed no movement of most projectiles. The only exception was the highly ferromagnetic Sintox Standard projectile.

When the highly ferromagnetic Sintox Standard projectile and the non-ferromagnetic MEN PEP 2.0 projectile were assessed in a pre-test, a comparison of CT scans that were obtained before and after 1-T MRI revealed displacement of the Sintox Standard projectile, which had been placed in the left masseter muscle. The scans provided evidence of cranial rotation of the tip of the projectile. A comparison of all CT scans that were performed before 1-T MRI and after 3-T MRI showed no further rotation or movement. When the main tests were performed with a different specimen (porcine head) on a different day, there was no rotational movement.

Images obtained during the tests are depicted in Fig. 2.

#### 3.2. Image quality

The images of all projectiles and fragments were evaluated in terms of the extent of artefacts and image quality. In addition, fragments of different sizes were examined in the case of the Sintox Standard projectile. An example of a complete evaluation is shown in Table 4, which provides the results obtained for a Zombie Max projectile. Images



Sintox Action 4 by RUAG Ammotec.



Gold Dot by Speer.



Zombie Max by Hornady.



9mm Luger by Magtech.



PEP 2.0 by MEN.



9mm Luger by Sellier & Bellot.



Sintox Standard by RUAG Ammotec.

**Fig. 1.** Photographs of the projectiles and fragments used during the tests.

**Table 2**  
Order of tests and description of the used projectiles.

| Test/porcine head | Left masseter muscle  | Right masseter muscle                                | Ferromagnetic attraction                   |
|-------------------|---|--|--|
| 1                 | Sintox Standard projectile  | MEN PEP 2.0 projectile                               | Yes on the left side, No on the right side |
| 2                 | Sintox Action 4 fragments   | Sintox Action 4 projectile                           | No   |
| 3                 | Speer Gold Dot fragments  | Speer Gold Dot projectile                            | No   |
| 4                 | Zombie Max fragments  | Zombie Max projectile                                | No   |
| 5                 | Magtech, 9 mm Luger, fragments                                    | Magtech, 9 mm Luger, projectile                      | No   |
| 6                 | MEN PEP 2.0 fragments   | MEN PEP 2.0 projectile                               | No   |
| 7                 | (No projectile or fragments)                                      | Sellier & Bellot, 9 mm Luger, projectile             | No   |
| 8                 | (No projectile or fragments)                                      | Sintox Standard projectile                           | Yes  |
| 9                 | Sintox Standard, all fragment sizes                               | (No projectile or fragments)                         | Yes  |
| 10                | (Removed)   | Sintox Standard, large fragment, approx. 1.5 cm long | Yes  |
| 11                | Sintox Standard, medium-sized fragment, approx. 5 mm long         | (Removed)  | Yes  |
| 12                | Sintox Standard, one of the smallest fragments, approx. 1 mm long | (Removed)  | Yes  |

**Table 3**  
Sequences and parameters tested.

| Standard protocol for the 1-T MRI scanner   |        |        |                       |
|---|--------|--------|-----------------------|
| 1-Tesla MRI                                 | TR     | TE     | Slice thickness in mm |
| T2 TSE sag                                  | 4540   | 99     | 5                     |
| T1 SE tra                                   | 515    | 8.2    | 6                     |
| T2 TIRM cor                                 | 9000   | 110    | 6                     |
| PD/T2 TSE tra                               | 3220   | 12/111 | 6                     |
| Diffusion EPI tra                           | 4600   | 98     | 5                     |
| T2 FL2D tra                                 | 766    | 26     | 6                     |
| Standard protocol for the 1.5-T MRI scanner |        |        |                       |
| 1.5-Tesla MRI                               | TR     | TE     | Slice thickness in mm |
| T2 TSE sag                                  | 11,430 | 103    | 4                     |
| PD/T2 TSE tra                               | 3040   | 10/104 | 5                     |
| T1 SE tra                                   | 590    | 10     | 5                     |
| T2 FLAIR cor                                | 9000   | 103    | 5                     |
| Diffusion EPI tra                           | 7700   | 88     | 5                     |
| SWI tra                                     | 49     | 40     | 2.5                   |
| Standard protocol for the 3-T MRI scanner   |        |        |                       |
| 3-Tesla MRI                                 | TR     | TE     | Slice thickness in mm |
| T2 TSE sag                                  | 8118.8 | 80     | 3                     |
| T2 FLAIR cor                                | 11,000 | 125    | 5                     |
| Dual TSE tra                                | 2000   | 10/80  | 4                     |
| Diffusion EPI tra                           | 4401.6 | 94     | 4                     |
| SWI tra                                     | 31     | 7.2    | 2                     |
| T1 FFE tra                                  | 418.5  | 4.6    | 4                     |

obtained during the tests are depicted in Fig. 3:

Table 5 provides an overview that compares and ranks the different types of projectiles from best to worst in terms of the results obtained for image quality and artefact size. The best results were achieved by Hornady's Zombie Max projectile and the poorest results were observed for the Sintox Standard projectile manufactured by RUAG Ammotec.

In general, our results show that non-ferromagnetic types of projectiles can be imaged more effectively than ferromagnetic types of projectiles. We found differences in image quality and artefact size between projectiles and projectile fragments of the same type. Sometimes projectiles and sometimes projectile fragments were imaged with fewer artefacts.

Artefacts and image quality were evaluated separately for

projectiles and projectile fragments on different sequences at 1 T, 1.5 T and 3 T.

The results for the image quality of projectiles, obtained for the sequences evaluated and ranked from best to worst are provided in Table 6.

The results for the image quality of projectile fragments, obtained for the sequences evaluated and ranked from best to worst are provided in Table 7.

As expected, our results confirm that SE and TSE sequences were superior to all other sequences (GRE/EPI) at all field strengths and were the least affected by metal-induced susceptibility artefacts. Gradient-echo sequences had considerably more artefacts. EPI and SWI sequences were associated with the poorest image quality and the largest

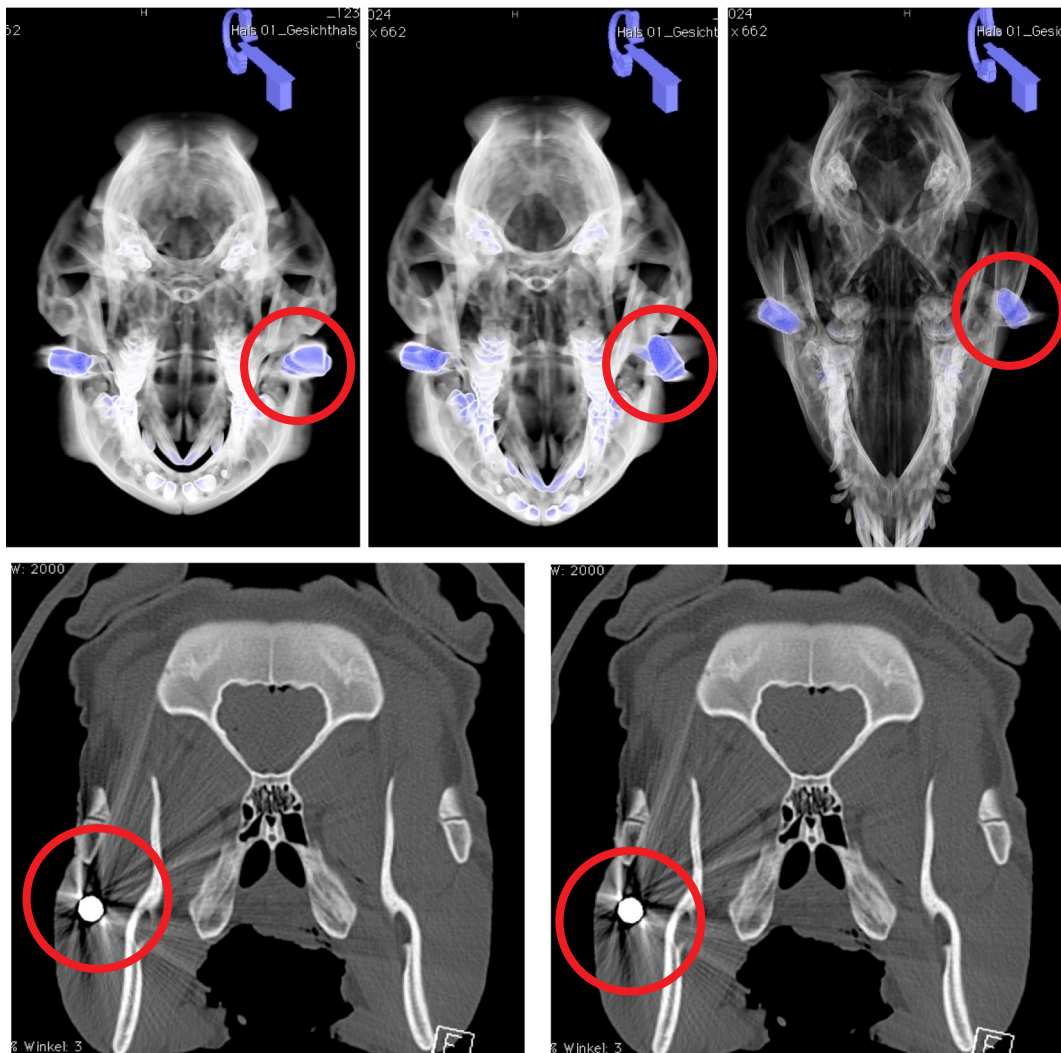


**Fig. 2.** Volume rendering technique (VRT) reconstruction of CT scans obtained during Test 1. Upper row: Left: pre-1-T MRI, middle: post-1-T MRI, right: post-3-T MRI. Note the movement of the highly ferromagnetic Sintox Standard projectile within the circles. Lower row: Coronal CT scans obtained during Test 8. Note the highly ferromagnetic Sintox Standard projectile lodged in the right masseter muscle (within the circles). Upper left: pre-1-T MRI, upper right, lower right: post-3-T MRI. In this test, there was no movement.

artefacts. As a result, these sequences are of no diagnostic utility regardless of whether projectiles or projectile fragments are magnetic or non-magnetic. (SE/TSE was found to be superior to GRE, which was superior to SWI/EPI.) Magnetic field strength had no relevant influence on image quality and the extent of artefacts. A higher field strength, in particular 3 T, did not lead to poorer results than lower field strengths (1 T and 1.5 T).

#### 4. Discussion

The behaviour of projectiles and projectile fragments in magnetic fields and during MRI has been a subject of research for many years. Previous studies focused on assessing the rotation and movement of projectiles in gel and gelatin blocks and included only a few MRI sequences. [2,5–7,11,12] These demonstrated considerable rotation and displacement of projectiles. These studies suggested that the extent of artefacts and movement depended on projectile composition.

Our study is the first to assess projectiles that were placed in muscle tissue and were then examined using all standard sequences for MRI of the central nervous system (CNS) following trauma. This allowed us to create realistic clinical conditions.

In general, ferromagnetic projectiles ( $n = 2$ ) and fragments were associated with poorer image quality and larger artefacts than non-ferromagnetic projectiles and fragments. The steel-jacketed Sintox Standard projectile (RUAG Ammotec), which is highly ferromagnetic, produced artefacts that were so large that MRI sequences did not provide any benefit for clinical practice. Substantial susceptibility artefacts made it almost impossible to accurately locate the projectile and to evaluate surrounding structures. Conventional military ammunition is designed in a similar way and therefore unsuitable for diagnostic MRI. Better imaging results were obtained for the Sintox Action 4 projectile (RUAG Ammotec), which is used by police and SWAT units. Although this projectile is made of a non-ferromagnetic copper alloy, it has minimal magnetic properties, which are probably the result of the

**Table 4**

Example of an evaluation of a projectile (Zombie Max).

Results for the extent of artefacts (AF) and image quality (IQ) under 1-T, 1.5-T and 3-T MRI conditions.

| Test 4 | MRI sequence      | Zombie Max |    |            |    |
|--------|-------------------|------------|----|------------|----|
|        |                   | Fragments  |    | Projectile |    |
|        |                   | AF         | IQ | AF         | IQ |
| 1 T    | T2 TSE sag        | 2          | A  | 2          | A  |
|        | T1 SE tra         | 1          | A  | 2          | A  |
|        | T2 TIRM cor       | 1          | A  | 1          | A  |
|        | PD/T2 TSE tra     | 1          | A  | 2          | A  |
|        | Diffusion EPI tra | 2          | B  | 1          | B  |
|        | T2 FL2D tra       | 2          | A  | 2          | A  |
| 1.5 T  | T2 TSE sag        | 1          | A  | 2          | A  |
|        | PD/T2 TSE tra     | 1          | A  | 2          | A  |
|        | T1 SE tra         | 1          | A  | 2          | A  |
|        | T2 FLAIR cor      | 2          | A  | 2          | A  |
|        | Diffusion EPI tra | 2          | B  | 2          | B  |
|        | SWI tra           | 3          | B  | 3          | B  |
| 3 T    | T2 TSE sag        | 2          | A  | 2          | A  |
|        | T2 FLAIR cor      | 1          | A  | 2          | A  |
|        | Dual TSE tra      | 1          | A  | 2          | A  |
|        | SWI tra           | 1          | B  | 2          | B  |
|        | T1 FFE tra        | 1          | A  | 2          | A  |
|        | Diffusion EPI tra | 1          | A  | 2          | B  |

presence of legally permissible amounts of metallic iron alloys. The quality of images with hunting projectiles was excellent. In general, these projectiles, which are non-magnetic, produced only minimal artefacts. It should be noted, however, that the results varied widely from minimal artefacts and excellent image quality to large artefacts (with a diameter of 3 to 5 cm) and moderate image quality. Interestingly, the images of projectiles and fragments of the same projectile showed qualitative differences. In some cases, projectiles were associated with larger artefacts and poorer image quality than their fragments. In other cases, the opposite was observed.

As expected, the best results in terms of image quality and artefacts were obtained using SE and TSE sequences. GRE and especially SWI and EPI sequences, which are particularly prone to susceptibility artefacts, provided images of poorer quality of both ferromagnetic and non-ferromagnetic projectiles and fragments. Whenever possible, MR imaging of patients with retained projectiles should therefore be performed using SE or TSE sequences. Eggert et al. [3] showed that image quality can be further improved using metal artefact reduction sequences (MARS). Interestingly, field strength did not influence image quality. The extent of artefacts that were observed at 3 T was similar to those at lower field strengths. This means that high field strength is not a criterion that excludes MRI in the presence of projectiles such as those investigated here.

In the present study, dislodgement of projectiles and projectile fragments during MRI was observed only for the highly magnetic Sintox Standard projectile (RUAG Ammotec), which is the standard ammunition for the P8 pistol used by the German Armed Forces. There was considerable movement of the projectile, which rotated to align in the direction of the magnetic field. This rotation, however, was not reproducible when the test was repeated. Translation and rotation usually occur where the magnetic field of a scanner is particularly strong, i.e. when a patient is moved into the gantry and exposed to the B<sub>0</sub> field. Dedini et al. [2] showed that ferromagnetic projectiles, which had been placed in gelatin blocks, exhibited considerable movement during MRI. The fact that the (masseter) muscle tissue that we used in our study has a much firmer texture than gelatin blocks probably explains why we detected movement of a projectile in only one test and why there was

no rotation in the majority of cases. Since the brain has a texture or consistency similar to that of gelatin, MRI must not be performed when a ferromagnetic projectile or fragment is located within brain tissue. By contrast, ferromagnetic projectiles may be examined by MR imaging when they are firmly incorporated into tissue, for example when they are lodged in bone or are encapsulated by fibrous tissue. Nevertheless, caution should be exercised with MRI. This imaging modality should not be used when projectiles are located near vital organs and should only be used on a case-by-case basis depending on the indication for MRI. These findings are in line with the results of a study conducted by Eshed et al. [4]

None of the other projectiles, which showed either a low level of magnetism (n = 1) or were non-ferromagnetic (n = 5), exhibited MRI-induced movement or dislodgement.

Heating of the projectiles or fragments appears not to play a significant role even at high specific absorption rates (SAR) as Martinez-del-Campo et al. [8] and Karacozoff et al. [7] showed in models.

So, the production and use of non-magnetic projectiles that are suitable for MRI should be favoured in the future, especially for standard weapons of police and security forces., knowing, that this will be hard to fulfil.

## 5. Conclusions

Our results suggest that gunshot injuries, esp. with retained projectiles and fragments, are no absolute contraindication for MRI, when the type of projectile and therefore the material composition is known.

While highly ferromagnetic projectiles and their fragments (such as those commonly used for military applications) not only cause substantial artefacts and do not provide any clinically relevant information, they are also associated with the potential risk of secondary displacement which can be fatal near vital structures. Non-ferromagnetic projectiles instead can provide good image quality with no harm for the patient.

While legally permissible amounts of metallic iron alloys may be present in ammunition where the product description does not mention iron, thus the exact knowledge of the behaviour of a projectile



**Fig. 3.** Images obtained during the tests:  
 Upper row: Transverse T1 (left) and SWI sequence (right) at 1.5 T;  
 A Zombie Max projectile (red circle, right masseter muscle) shows larger artefacts than fragments of the same type of projectile (green circle, left masseter muscle) and SWI- sequence more artefacts than SE- sequence. Left T1 SE; right SWI  
 Middle row: Coronal T2 FLAIR sequence at 3 T.  
 Left: a MEN PEP 2.0 projectile lodged in the right masseter muscle and a highly ferromagnetic Sintox Standard projectile located in the left masseter muscle with substantial susceptibility artefacts and signal voids.  
 Right: a MEN PEP 2.0 projectile lodged in the right masseter muscle and projectile fragments of the same type on the contralateral side. Good image quality.  
 Lower row: Coronal T2 FLAIR (left) and transverse SWI- sequence at 3 T  
 Severe susceptibility artefacts caused by a highly ferromagnetic projectile (Sintox Standard) in the right masseter muscle. (For interpretation of the references to colour in this figure legend, the reader is referred to the web version of this article.)

(provided by our and further studies) is necessary before an MRI in the acute stage of injury can be performed. We aim to create an atlas of projectiles and their characteristics concerning MRI compability and hope to motivate manufactures to create MRI compatible ammunition in the future, especially for standard weapons of police and security forces, knowing that this will be hard to fulfil.

Parts of this article are based on the Dissertation of M. Wafa: “Beurteilung von Artefaktmaß, Bildqualität sowie Bewegungs- und Rotationsverhalten von Projektilen des Kalibers 9 × 19 mm und deren Projekttilfragmenten im MRT der Stärke 1, 1.5 und 3 T.” (University of Ulm, 2018).

**Abbreviations**

|       |                                     |
|-------|-------------------------------------|
| AF    | artefact                            |
| CT    | computed tomography                 |
| cor   | coronal                             |
| EPI   | echo-planar imaging                 |
| FFE   | fast field echo                     |
| FLAIR | fluid-attenuated inversion recovery |
| FL2D  | gradient echo sequence              |
| PD    | proton density                      |

|      |                                    |
|------|------------------------------------|
| IQ   | image quality                      |
| MARS | metal artefact reduction sequence  |
| MRI  | magnetic resonance imaging         |
| SE   | spin-echo                          |
| T    | Tesla                              |
| T1   | T1-weighted sequence               |
| T2   | T2-weighted sequence               |
| TE   | echo time                          |
| TIRM | turbo inversion recovery magnitude |
| TR   | repetition time                    |
| tra  | transverse                         |
| TSE  | turbo spin-echo                    |
| sag  | sagittal                           |
| SAR  | specific absorption rate           |
| SWAT | special weapons and tactics        |
| SWI  | susceptibility-weighted Imaging    |
| VRT  | volume rendering technique         |

**Declarations of interest**

None.

**Table 5**  
Overview of data on the projectiles used and the results for image quality and extent of artefacts.

| Projectile                   | Manufacturer     | Composition                           | Type of gun            | Type of projectile | Use                                     | Magnetism  | Mean extent of artefacts | Mean image quality | Ranking from best to worst |
|------------------------------|------------------|---------------------------------------|------------------------|--------------------|---|------------|--------------------------|--------------------|----------------------------|
| Zombie Max                   | Homady           | Copper jacket, lead core              | Revolver               | Hollow point       | Hunters                                 | No         | 1–2                      | A–B                | 1                          |
| Magtech, 9 mm Luger          | Magtech          | Copper jacket, lead core              | Pistol                 | Fully jacketed     | Hunters                                 | No         | 1–2                      | A–B                | 1                          |
| Sellier & Bellot, 9 mm Luger | Sellier & Bellot | Lead, solid                           | Pistol                 | Lead, round-nosed  | Hunters                                 | No         | 2                        | A–B                | 2                          |
| Speer Gold Dot               | Speer            | Copper, solid                         | Pistol                 | Hollow point       | Hunters, police                         | No         | 2–3                      | A–B                | 3                          |
| MEN PEP 2.0                  | MEN              | Copper, solid                         | Pistol                 | Semi-jacketed      | Police                                  | No         | 2–3                      | A–B                | 4                          |
| Sintox Action 4              | RUAG             | Copper alloy, solid                   | Pistol, submachine gun | Semi-jacketed      | Police, SWAT teams                      | Low level  | 3–4                      | B–C                | 5                          |
| Sintox Standard              | RUAG             | Nickel-plated steel jacket, lead core | Pistol, submachine gun | Fully jacketed     | Police, SWAT teams, German armed forces | High level | 4                        | C                  | 6                          |

**Table 6**

| Order of image quality for projectiles | Sequences   |
|--|---|
| 1                                      | T2 TSE sag (1 T–3 T)                                    |
| 2                                      | T2 TIRM cor/T2 Flair cor (1.5 T–3 T)/dual TSE tra (3 T) |
| 3                                      | T1 SE tra (1 T–1.5 T) /PD/T2 TSE tra (1 T, 1.5 T)       |
| 4                                      | T1 FFE tra (3 T)  |
| 5                                      | T2 FL2D tra (1 T)                                       |
| 6                                      | SWI tra (1.5 T, 3 T)                                    |
| 7                                      | Diffusion EPI tra (1 T–3 T)                             |

**Table 7**

| Order of image quality for projectile fragments | Sequences   |
|---|---|
| 1   | T2 TSE sag (1 T–3 T)/T1 SE tra (1 T, 1.5 T)/T2 Flair cor (3 T)/dual TSE tra (3 T) |
| 2   | T2 TIRM cor (1 T) (T2 Flair cor (1.5 T))/PD/T2 TSE tra (1 T, 1.5 T)               |
| 3   | T1 FFE tra (3 T)/T2 FL2D tra (1 T)  |
| 4   | Diffusion EPI tra (1 T–3 T)   |
| 5   | SWI tra (1.5 T, 3 T)  |

**References**

- [1] Adam O, Mac Donald CL, Rivet D, Ritter J, May T, Barefield M, et al. Clinical and imaging assessment of acute combat mild traumatic brain injury in Afghanistan. *Neurology* 2015;85:219–27.
- [2] Dedini RD, Karacozoff AM, Shellock F, Xu D, McClellan RT, Pekmezci M. MRI issues for ballistic objects: information obtained at 1.5-, 3- and 7-Tesla. *Spine J* 2013;13:815–22.
- [3] Eggert S, Kubik-Huch RA, Klarhöfer M, Peters A, Bolliger SA, Thali MJ, et al. Fairly direct hit! Advances in imaging of shotgun projectiles in MRI. *Eur Radiol* 2015;25:2745–53.
- [4] Eshed I, Kushnir T, Shabshin N, Konen E. Is magnetic resonance imaging safe for patients with retained metal fragments from combat and terrorist attacks? *Acta Radiol* 2010;51:170–4.
- [5] Hess U, Harms J, Lanzl I, Wilhelm T, Gräfin v. Einsiedel H. The radiological diagnosis of an intraorbital bullet projectile. *Radiologe* 2000;40:404–7.
- [6] Hess U, Harms J, Schneider A, Schleaf M, Ganter C, Hannig C. Assessment of gunshot bullet injuries with the use of magnetic resonance imaging. *J Trauma-Inj Int Crit Care* 2000;49:704–9.
- [7] Karacozoff AM, Pekmezci M, Shellock FG. Armor-piercing bullet: 3-T MRI findings and identification by a ferromagnetic detection system. *Mil Med* 2013;178:380–5.
- [8] Martinez-del-Campo E, Rangel-Castilla L, Soriano-Baron H, Theodore N. Magnetic resonance imaging in lumbar gunshot wounds: an absolute contraindication? *Neurosurg Focus* 2014;37:1–7.
- [9] n-tv.de, dsi. <http://www.n-tv.de/politik/Auch-legale-Waffen-toeten-article12090366.html>, Accessed date: 4 March 2016.
- [10] Reginelli A, Russo A, Maresca D, Martiniello C, Cappabianca S, Brunese L. Imaging assessment of gunshot wounds. *Semin Ultrasound CT MRI* 2014;36:57–67.
- [11] Smith AS, Hurst GC, Duerk JL, Diaz PJ. MR of ballistic materials: imaging artifacts and potential hazards. *Am Soc Neuroradiol* 1991;12:567–72.
- [12] Teitelbaum GP, Yee CA, Van Horn DD, Kim HS, Colletti PM. Metallic ballistic fragments: MR imaging safety and artifacts. *Radiology* 1990;175:855–9.
- [13] TraumaRegister DGU. Committee on emergency medicine, intensive care and trauma management of the German Trauma Society (Sektion NIS). *Int J Care Injured* 2014;45S:14–9.